



Photonics-based radio frequency self-interference cancellation for radio-over-fiber systems

XIAOPENG HU,¹ DAN ZHU,^{1,2} HAI XIAO,¹ AND SHILONG PAN^{1,*}

¹Key Laboratory of Radar Imaging and Microwave Photonics, Ministry of Education, Nanjing University of Aeronautics and Astronautics, Nanjing 210016, China

²e-mail: danzhu@nuaa.edu.cn

*Corresponding author: pans@nuaa.edu.cn

Received 29 April 2022; revised 16 June 2022; accepted 27 June 2022; posted 25 July 2022; published 10 August 2022

A photonics-based radio frequency (RF) self-interference cancellation approach for radio-over-fiber (RoF) systems is proposed and demonstrated. An intermediate frequency (IF) signal and a local oscillator (LO) signal are separately modulated to a pair of optical carriers with orthogonal polarization states in the central station. The generated optically carried RF signal is then transmitted to remote base stations over fibers. After performing photodetection at the two outputs of the polarization beam splitter (PBS), a pair of upconverted RF signals with inverse phases are generated. One is used as the transmitted signal, while the other is used as the reference signal for the self-interference cancellation. In this way, the phase inversion between them is realized in the optical domain. In addition, the adjustments with the time delay and the amplitude of the reference signal are both achieved in the optical domain, guaranteeing the self-interference cancellation in a wide bandwidth. Meanwhile, the independent optical system for self-interference cancellation is avoided, simplifying the complex hardware requirements with the base stations. The cancellation depths of 33, 30, and 22 dB over 0.5-, 1-, and 3-GHz bandwidths are experimentally achieved, respectively. The ranging and imaging functions of a frequency modulated continuous wave (FMCW) radar system using the established self-interference cancellation structure are experimentally verified. © 2022 Optica Publishing Group

<https://doi.org/10.1364/OL.462681>

The in-band full-duplex radio-over-fiber (RoF) techniques are of great importance in future distributed RF systems for radar, wireless communication, and electronic warfare applications [1–4]. However, the receiver frontend will inevitably receive the unwanted signal leaked from its transmitter [5]. The so-called self-interference overlaps with the wanted RF signals in the spectrum and thus cannot be removed through filtering. A self-interference cancellation function is urgently needed.

To realize the self-interference cancellation, an additional chain carrying the reference signal is introduced to subtract the self-interference [6]. The cancellation performances, including the bandwidth and the cancellation depth, depend on how well the reference signal matching with the self-interference signal in terms of amplitude, time delay, and phase. Photonics-based

self-interference cancellation approaches have been reported, due to advantages in working bandwidth, low transmission loss, and so on introduced by photonics [7–18]. For the previous works, the main point is to achieve the phase inversion between the self-interference signal and the reference signal based on photonic approaches. It can be achieved by introducing counter-phase modulations [7–11], balanced photodetection [12–14], cross-gain modulation [15], and microwave photonic phase shifters [16–18]. However, when applied in RoF systems, the operations of amplitude and time delay matching being conducted in the electrical domain will still limit the working bandwidth [8–10]. To solve this problem, in Refs. [11–13], the amplitude, time delay matching, and phase inversion are all realized in the optical domain. However, no less than two light sources and electro-optic modulators (EOMs), or a complex dual-polarization modulator, are needed, making the remote base stations complex and costly. Furthermore, for actual applications, the power of the self-interference signal is usually much higher than the signal of interest. For the previous photonics-based approaches, the received RF signal needs to be amplified before the cancellation structure. The self-interference signal with high power will saturate the RF amplifier and deteriorate the amplification of the signal of interest [19,20].

Recently, we proposed a photonics-based self-interference cancellation approach for RoF systems [21]. However, only the preliminary experimental results have been reported. In this Letter, comprehensive investigations and discussions are performed. In the central office, a pair of optical carriers with orthogonal polarization states are used to modulate the intermediate frequency (IF) signal and the local oscillator (LO) signal, respectively. In the base station, a pair of upconverted RF signals with inverse phases are generated after performing the photodetection at the two outputs of the polarization beam splitter (PBS). One of the RF signals is used as the transmitted signal, while the other one is used as the reference signal. The time delay and amplitude matching between the reference signal and the self-interference signal is accomplished in the optical domain. By simply combining the reference signal and the received signal, the self-interference cancellation is achieved. There is no need for an independent optical system to achieve the self-interference cancellation at the base stations, simplifying the complex hardware requirements. A proof-of-concept experiment is taken. The cancellation depths of 33, 30, and 22 dB over 0.5-, 1-, and 3-GHz

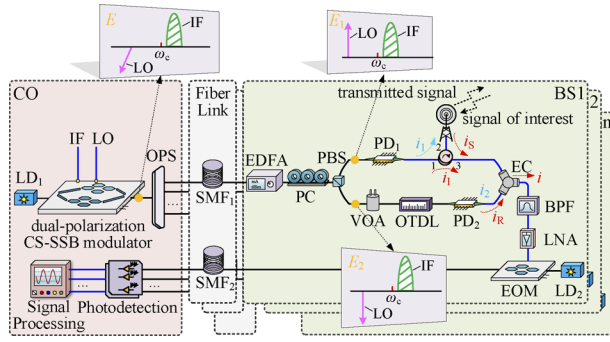


Fig. 1. Proposed photonics-based self-interference cancellation scheme. CO, central office; CS-SSB, carrier-suppressed single-sideband; LO, local oscillator; LD, laser diode; IF, intermediate frequency; OPS, optical power splitter; SMF, single-mode fiber; BS, base station; EDFA, erbium-doped fiber amplifier; PC, polarization controller; PBS, polarization beam splitter; PD, photodetector; EC, electrical coupler; BPF, bandpass filter; OTDL, optical time delay line; LNA, low-noise amplifier; VOA, variable optical attenuator; EOM, electro-optic modulator.

bandwidths are achieved, respectively. By using the proposed self-interference cancellation structure, the ranging and imaging functions of a frequency modulated continuous wave (FMCW) radar system are also experimentally verified.

The proposed photonics-based self-interference cancellation scheme for RoF systems is illustrated in Fig. 1. It consists of the central office, the fiber transmission link, and the remote base stations. In the central office, by using a dual-polarization carrier-suppressed single sideband (CS-SSB) modulator, an IF signal ω_{IF} and an LO signal ω_{LO} are modulated to the orthogonally polarized optical carriers with the angular frequency of ω_c , respectively. The output optical field of the dual-polarization CS-SSB modulator is

$$E = \begin{bmatrix} E_x \\ E_y \end{bmatrix} = \begin{bmatrix} ae^{j(\omega_c \pm \omega_{IF})t} \\ be^{j(\omega_c \mp \omega_{LO})t} \end{bmatrix}, \quad (1)$$

where a and b are the corresponding optical sideband amplitudes. The polarization-multiplexed optical signal is then divided into multiple parts by an optical power splitter, which are sent to different remote base stations through fiber transmission. In each base station, the optical signal is divided into two parts by using a polarization controller (PC) followed by a PBS, with the expression:

$$\begin{cases} E_1 = E_x \cos \theta + E_y \sin \theta \\ E_2 = E_x \cos(\theta + \frac{\pi}{2}) + E_y \sin(\theta + \frac{\pi}{2}). \end{cases} \quad (2)$$

The value of θ can be tuned by adjusting the PC. When $\theta = 45^\circ$, the two outputs can be rewritten as

$$\begin{cases} E_1 = \frac{\sqrt{2}}{2}(E_x + E_y) = \frac{\sqrt{2}}{2}[ae^{j(\omega_c \pm \omega_{IF})t} + be^{j(\omega_c \mp \omega_{LO})t}] \\ E_2 = \frac{\sqrt{2}}{2}(E_x - E_y) = \frac{\sqrt{2}}{2}[ae^{j(\omega_c \pm \omega_{IF})t} - be^{j(\omega_c \mp \omega_{LO})t}]. \end{cases} \quad (3)$$

After photodetection, two up-converted RF signals with inverse phases are generated, which can be expressed as

$$\begin{cases} i_1 = \sqrt{2}ab\mathfrak{R} \cos(\omega_{LO} + \omega_{IF})t \\ i_2 = -\sqrt{2}ab\mathfrak{R} \cos(\omega_{LO} + \omega_{IF})t, \end{cases} \quad (4)$$

where \mathfrak{R} is the responsivity of the photodetectors (PDs). The RF signal i_1 in the upper branch is used as the transmitted signal. The received signal consists of the desired signal of interest i_s and the unwanted self-interference signal i_i . Here, $i_s = d \cos \omega_s t$, where d and ω_s are the amplitude and the angular frequency, respectively. The self-interference can be regarded as a replica of the transmitted signal with time delay and amplitude attenuation,

$$i_i = \sqrt{2}aba\mathfrak{R} \cos(\omega_{LO} + \omega_{IF})(t - \tau), \quad (5)$$

where α and τ donate the attenuation and the time delay with the leakage, respectively. The RF signal i_2 in the lower branch is used as the reference signal. In this branch, a variable optical attenuator (VOA) is incorporated to adjust the amplitude of the reference signal, while an optical time delay line (OTDL) is used to tune the time delay. The reference signal is given as

$$i_r = -\sqrt{2}aba_{VOA}\mathfrak{R} \cos(\omega_{LO} + \omega_{IF})(t - \tau_{OTDL}), \quad (6)$$

where α_{VOA} represents the attenuation coefficient of the VOA, and τ_{OTDL} represents the time delay introduced by the OTDL. By combining the received RF signal and the reference signal, the output from the electrical coupler is written as

$$\begin{aligned} i &= i_s + i_i + i_r \\ &= d \cos \omega_s t + \sqrt{2}aba\mathfrak{R} \cos(\omega_{LO} + \omega_{IF})(t - \tau) \\ &\quad - \sqrt{2}aba_{VOA}\mathfrak{R} \cos(\omega_{LO} + \omega_{IF})(t - \tau_{OTDL}). \end{aligned} \quad (7)$$

The VOA and the OTDL are adjusted to make $\alpha_{VOA} = \alpha$ and $\tau_{OTDL} = \tau$. Thus, it can be achieved that $i = d \cos \omega_s t$. In this way, the effective suppression of the self-interference signal is achieved, and only the signal of interest is left. After being filtered by the bandpass filter (BPF) and amplified by the LNA, the signal of interest is modulated to the optical carrier and sent to the central office for further processing.

Experiments are taken with the setup shown in Fig. 1. An optical carrier with a 1550.12-nm wavelength and an 18-dBm power is produced by a laser diode (LD, Teraxion PS-NLL). The dual-polarization CS-SSB modulator is achieved by using a dual polarization quadrature phase shift keying (DP-QPSK) modulator (Fujitsu FTM7977) together with two 90-degree electrical hybrids. The 3-dB bandwidth and the half-wave voltage of the DP-QPSK modulator are 23 GHz and 3.5 V, respectively. The signal of interest and the IF signal are produced by a four-channel arbitrary waveform generator (Keysight M8195A, 65 GSA/s). The LO signal is generated from a microwave signal generator (Rohde & Schwarz SMA100B, 8 kHz–67 GHz). The single-mode fiber (SMF) for the downlink transmission has a length of 37 km. The 3-dB bandwidth and the responsivity of the PDs (CETC44 GD45216S) are 20 GHz and 0.8 A/W, respectively. The attenuation range of the VOA (Ziguan) is 0–40 dB. The delay adjusting range of the OTDL (General Photonics) is 660 ps. The electrical coupler (EC, Talent Microwave RS2W20400-K) has a phase unbalance and an amplitude unbalance within ± 1 deg and ± 0.2 dB over a 20-GHz bandwidth. The electrical spectra are monitored by an electrical spectrum analyzer (R&S FSV40, 10 Hz–40 GHz) with a resolution of 500 kHz. The optical spectra are monitored by an optical spectrum analyzer (Apex AP2040D) and the resolution is 5 MHz.

First, the wideband self-interference cancellation performance of the proposed system is verified. A linear frequency modulated (LFM) signal with a 500-MHz bandwidth is used as the IF signal. It has a center frequency of 2.75 GHz and a power

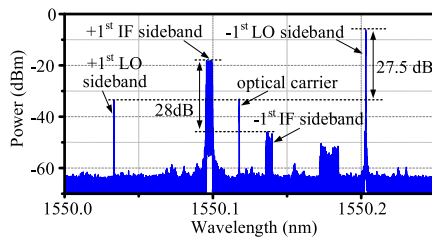


Fig. 2. Measured optical spectra at the output of the dual-polarization CS-SSB modulator when the IF signal has a 500-MHz bandwidth.

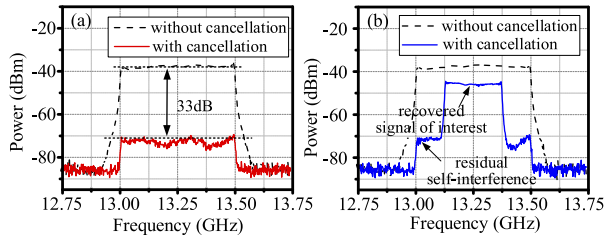


Fig. 3. Experimentally obtained electrical spectra of the received RF signal with and without taking the self-interference cancellation when the signal of interest is (a) disabled and (b) enabled. The bandwidths of the signal of interest and the IF signal are 250 and 500 MHz, respectively.

of 15 dBm. Meanwhile, the LO signal is 10.5 GHz and the power is 18 dBm. The signal of interest is set to be an LFM signal centered at 13.25 GHz with a bandwidth of 250 MHz. Figure 2 shows the optical spectrum at the output of the dual-polarization CS-SSB modulator. As can be seen, the +1st-order sideband of the optically carried IF signal and the -1st-order sideband of the optically carried LO signal are retained. Meanwhile, the unwanted optical sidebands are well suppressed and the suppression ratios are larger than 27 dB. The effective suppression with the unwanted optical sidebands and the optical carrier guarantees the good suppression with the unwanted mixing spurs at PD1. For simplicity, the transmitting/receiving antenna and the RF circulator are not applied here. The output of PD₁ is used as the self-interference signal. It is combined with the signal of interest and then sent to one input port of the electrical coupler. The cancellation results are measured at the output of the electrical coupler. Figure 3(a) shows the measured electrical spectra of the received RF signal with and without self-interference cancellation when the signal of interest is disabled. When disconnecting the reference signal, the received signal centered at 13.25 GHz without cancellation is plotted as the black dashed line. When the reference signal is connected, the received signal with cancellation is plotted as the red solid line. The cancellation depth of 33 dB can be observed over the whole 500-MHz bandwidth. The signal of interest is then enabled to investigate the system performance in the full-duplex operation, and the cancellation result is shown in Fig. 3(b). The signal of interest is successfully recovered from the self-interference and the cancellation performance remains unchanged.

The self-interference cancellation for RF signals with different bandwidths is also implemented. For the condition of 1-GHz bandwidth, the carrier frequencies of the IF signal and the LO signal are set to 2.5 and 11 GHz, respectively, while for the condition of a 3-GHz bandwidth, the IF signal is tuned to have

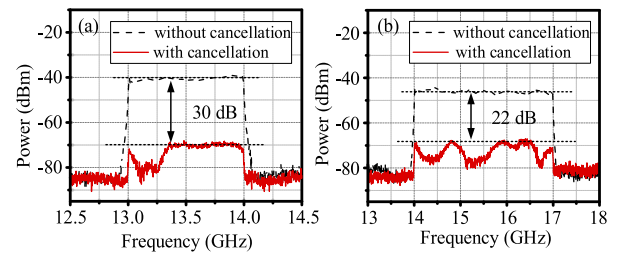


Fig. 4. Experimentally obtained electrical spectra of the received RF signal with and without taking the self-interference cancellation, when the IF signal has a bandwidth of (a) 1 GHz and (b) 3 GHz, respectively.

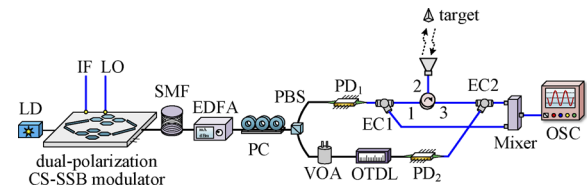


Fig. 5. Experimental setup of a frequency modulated continuous wave (FMCW) radar transceiver application. LD, laser diode; LO, local oscillator; IF, intermediate frequency; CS-SSB, carrier-suppressed single-sideband; SMF, single-mode fiber; EDFA, erbium-doped fiber amplifier; PBS, polarization beam splitter; PC, polarization controller; VOA, variable optical attenuator; OTDL, optical time delay line; EC, electrical coupler; PD, photodetector; OSC, oscilloscope.

a center frequency of 5 GHz and the LO signal is tuned to be 10.5 GHz. The corresponding cancellation results are shown in Figs. 4(a) and 4(b), respectively. The self-interference cancellation depths of 30 and 22 dB are achieved for the 1- and 3-GHz bandwidth conditions, respectively.

Then, the performance of the established self-interference cancellation structure in a radar transceiver application is investigated with the experimental setup shown in Fig. 5. The transmitted signal is an LFM signal with a bandwidth of 500 MHz and a center frequency of 13.25 GHz. A corner reflector is used as the target. The received RF signal contains the signal of interest (the echo signal reflected from the target) and the self-interference signal (the RF circulator's leakage). It is mixed with a part of the transmitted signal to realize de-chirp processing. The de-chirped output is sampled by a real-time oscilloscope (Agilent DSOX92504A) with a sampling rate of 50 MSa/s. First, the target is placed 0.5-m away from the antenna. After performing the fast Fourier transform with the de-chirped output, the range profiles are obtained and shown in Fig. 6(i), and Fig. 6(ii) shows the corresponding imaging results. Without the self-interference cancellation, two peaks corresponding to the self-interference and the target can be observed in the range profiles, as shown in Fig. 6 (a-i). When the self-interference cancellation is taken, only the peak corresponding to the target remains, as shown in Fig. 6 (b-i). Only the target information is preserved in the imaging results by taking the self-interference cancellation, and the comparison is given in Figs. 6 (a-ii) and 6 (b-ii). It should be noted that the peak corresponding to the target is located at approximately 1.7 m, instead of the actual 0.5 m. The inconsistency is caused by the non-zero reference point introduced by the signal transmission path differences.

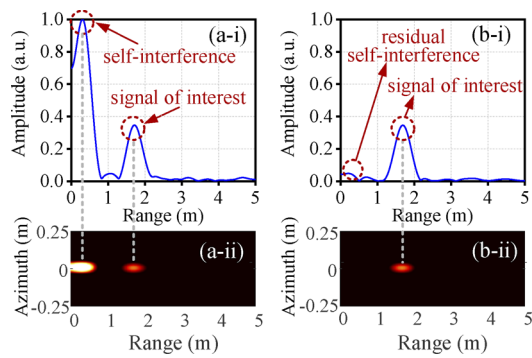


Fig. 6. (i) Range profiles and (ii) imaging results (a) without and (b) with the photonics-based self-interference cancellation when the target is placed 0.5-m away from the antenna.

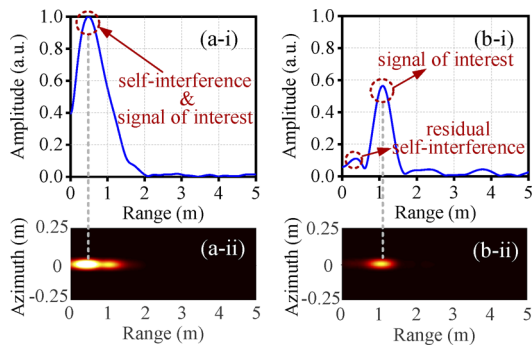


Fig. 7. (i) Range profiles and (ii) imaging results (a) without and (b) with the photonics-based self-interference cancellation when the target is placed 0.1-m away from the antenna.

Then the target is placed 0.1-m away from the antenna, and the range profiles and the corresponding imaging results are plotted in Fig. 7(i) and Fig. 7(ii), respectively. In Fig. 7(a-i), without the self-interference cancellation, since the distance between the target and the antenna is very close, the peaks corresponding to the target and the self-interference are overlapped. Meanwhile, the imaging results of the target and the self-interference cannot be distinguished, as shown in Fig. 7(a-ii). By taking the self-interference cancellation, the target can be observed clearly, as shown in Figs. 7(b-i) and Fig. 7(b-ii).

In conclusion, a photonics-based self-interference cancellation approach has been demonstrated for RoF systems. The phase inversion, the time delay, and the amplitude matching between the self-interference signal and the reference signal are all taken in the optical domain to realize the wideband self-interference cancellation. Meanwhile, the independent optical system for self-interference cancellation is avoided to simplify the base stations. Furthermore, as compared with the previous works, the RF signal amplification can be taken after the can-

cellation structure. In this way, the amplification efficiency and the system performance can be guaranteed. The power budget can be further reduced by using a DP-QPSK modulator with a smaller insert loss and a lower half-wave voltage. The separate fiber transmissions can be further improved by using a shared fiber for both downlink and uplink transmissions. The amplitude and phase response of the EC should be consistent to guarantee the system performance. The proposed approach can be applied to allow in-band full-duplex operations in future distributed RF systems, such as radar, wireless communication, and so on.

Funding. National Natural Science Foundation of China (61971222).

Disclosures. The authors declare no conflicts of interest.

Data availability. Data underlying the results presented in this paper are not publicly available at this time but may be obtained from the authors upon reasonable request.

REFERENCES

- Z. Zhang, X. Chai, K. Long, A. V. Vasilakos, and L. Hanzo, *IEEE Commun. Mag.* **53**, 128 (2015).
- D. Zhu and S. Pan, *J. Lightwave Technol.* **38**, 3076 (2020).
- A. T. Le, Y. Nan, L. C. Tran, X. Huang, Y. J. Guo, and Y. Vardaxoglou, in *IEEE 88th Vehicular Technology Conference* (IEEE, 2018), p. 1.
- J. Marin, M. Turunen, M. Bernhardt, and T. Riihonen, in *International Conference on Military Communication and Information Systems* (IEEE, 2021), p. 1.
- H. Alves, T. Riihonen, and H. A. Suraweera, *Full-Duplex Communications for Future Wireless Networks* (Springer, 2020).
- A. Sabharwal, P. Schniter, D. Guo, D. W. Bliss, S. Rangarajan, and R. Wichman, *IEEE J. Select. Areas Commun.* **32**, 1637 (2014).
- J. Suarez, K. Kravtsov, and P. R. Prucnal, *IEEE J. Quantum Electron.* **45**, 402 (2009).
- Y. Chen and S. Pan, *Opt. Lett.* **43**, 3124 (2018).
- Y. Chen, *J. Lightwave Technol.* **38**, 4618 (2020).
- H. Song, X. Li, Y. Zhang, L. Huang, M. Cheng, D. Liu, and L. Deng, *J. Lightwave Technol.* **40**, 511 (2022).
- P. Li, L. Yan, J. Ye, X. Feng, X. Zou, B. Luo, W. Pan, T. Zhou, and Z. Chen, *J. Lightwave Technol.* **38**, 1178 (2020).
- J. Wang, H. Yu, Z. Zhao, Z. Zhang, and J. Liu, *Appl. Opt.* **60**, 3021 (2021).
- Z. Zhu, C. Gao, S. Zhao, T. Zhou, G. Wang, H. Li, and Q. Tan, *J. Lightwave Technol.* **40**, 655 (2022).
- M. P. Chang, M. Fok, A. Hofmaier, and P. R. Prucnal, *IEEE Microw. Wireless Compon. Lett.* **23**, 99 (2013).
- M. P. Chang, C. Lee, B. Wu, and P. R. Prucnal, *IEEE Photon. Technol. Lett.* **27**, 1018 (2015).
- Y. Xiang, G. Li, and S. Pan, *Opt. Express* **25**, 21259 (2017).
- D. Zhu, X. Hu, W. Chen, D. Ben, and S. Pan, *Opt. Lett.* **44**, 5541 (2019).
- X. Hu, D. Zhu, L. Li, and S. Pan, *J. Lightwave Technol.* **40**, 1989 (2022).
- K. E. Kolodziej, S. Yegnanarayanan, and B. T. Perry, *IEEE Trans. Microwave Theory Tech.* **67**, 2076 (2019).
- K. E. Kolodziej, S. Yegnanarayanan, and B. T. Perry, *IEEE Trans. Microwave Theory Tech.* **67**, 4005 (2019).
- X. Hu, D. Zhu, and S. Pan, in *International Topical Meeting on Microwave Photonics* (IEEE, 2021), paper We 1.3.